

Raman Scattering in Charge Ordered $\text{Pr}_{0.63}\text{Ca}_{0.37}\text{MnO}_3$: Anomalous Temperature Dependence of Linewidth

RAJEEV GUPTA¹ (*), G. VENKETESWARA PAI² (**), A. K. SOOD¹(***),
T. V. RAMAKRISHNAN² and C. N. R. RAO³

¹ *Department of Physics, Indian Institute of Science, Bangalore - 560012, India.*

² *Centre for Condensed Matter Theory, Department of Physics, Indian Institute of Science, Bangalore - 560012, India.*

³ *CSIR Centre for Excellence in Chemistry, Jawaharlal Nehru Centre for Advanced Scientific Research, Jakkur P.O, Bangalore - 560064, India.*

PACS. 75.30.Vn – Colossal Magnetoresistance.

PACS. 78.30.-j – Infrared and Raman spectra.

PACS. 72.10.Di – Scattering of phonons, magnons, and other nonlocalized excitations.

Abstract. – We report on the evolution of the Raman-active A_g phonon modes in the charge-ordered manganite $\text{Pr}_{0.63}\text{Ca}_{0.37}\text{MnO}_3$ as a function of temperature from 300K to 25K. Our studies reveal that the linewidths of the $A_g(2)$ and $A_g(4)$ phonons increase as temperature decreases. This anomalous temperature dependence of phonon lineshapes, seen for the first time in charge ordered manganites, can be quantitatively understood in terms of a strong spin-phonon coupling involving t_{2g} spins and A_g phonons.

The recent upsurge of interest in doped manganites exhibiting colossal magnetoresistance has fuelled a lot of interesting questions regarding the role of spin, orbital and lattice degrees of freedom and the interplay amongst them [1]. These systems of the form $A_{1-x}A'_x\text{MnO}_3$, where A is a trivalent rare earth ion (*e.g.*, La, Pr, Nd) and A' is a divalent ion (*e.g.*, Ca, Sr, Pb) show a rich phase diagram depending on the tolerance factor and the amount of doping x which in turn controls the ratio of Mn^{3+} to Mn^{4+} . The essential ingredients for understanding their electronic properties are the double-exchange(DE) mechanism [2] and the polaron formation due to the Jahn-Teller(JT) effect [3]. In the case of systems where the weighted average A-site cation radius is small, the system also shows charge ordering (CO), *i.e.*, real space ordering of Mn^{3+} and Mn^{4+} ions at low temperatures [4]. The CO state becomes stable when the repulsive Coulomb interaction between the carriers or the cooperative JT effect dominates over the kinetic energy of carriers. In such situations there is a strong competition between the DE interaction which favours ferromagnetism (FM), and CO which favours antiferromagnetism (AF) via the coupling between the background t_{2g} ($S = 3/2$) spins.

(*) Present Address : 104 Davey Laboratory, Pennsylvania State University, University Park, PA 16802, USA

(**) Present Address : The Abdus Salam International Centre for Theoretical Physics, Strada Costiera 11, 34100 Trieste, Italy

(***) Email : [rajeev, venkat, asood, tvrama] @physics.iisc.ernet.in ; cnrrao@jncasr.ac.in

The system under study, $\text{Pr}_{1-x}\text{Ca}_x\text{MnO}_3$, shows a rich phase diagram as a function of doping and temperature and has been studied using a variety of probes like resistivity [5], magnetization and neutron diffraction [6]. In the temperature range $T > T_{CO}$ (~ 240 K) the system is a paramagnetic insulator. In dc magnetic susceptibility, a large peak is observed at T_{CO} followed by a relatively small peak at T_N . The peak at T_{CO} is attributed to ferromagnetic correlations [7]. The system further undergoes a transition at $T_N \sim 175$ K to the charge-exchange (CE) type antiferromagnetic insulator (AFI). The CE type structure for $x < 0.5$ is different from what is present in systems with $x = 0.5$. In this so called "pseudo-CE" structure the zig-zag FM chains in the ab plane are FM aligned along the c -axis [7]. This is unlike the CE structure where the layers in the ab plane are aligned antiferromagnetically along c . Further lowering of temperature below 50 K leads to another transition which can be understood either as a canted antiferromagnetic state [6] or as a mixture of ferromagnetic domains (or clusters) in an antiferromagnetic background.

In this letter we report our Raman studies on well characterized, high-quality single crystals of $\text{Pr}_{0.63}\text{Ca}_{0.37}\text{MnO}_3$ [8] as a function of temperature from 300 K to 25 K. There are many Raman studies on manganites in recent times covering both the vibrational [9–13] and electronic Raman scattering [14] across the metal-insulator transition. In a recent work on polycrystalline $\text{Pr}_{0.65}\text{Ca}_{0.35}\text{MnO}_3$ [15], temperature dependence of the modes at 475 and 610 cm^{-1} was studied and the splitting of these modes below T_{CO} was attributed to the folding of the Brillouin zone in the CO state. In another Raman study [16], the effect of A-site substitution on the $A_g(2)$ mode was discussed. However, the linewidths have not been discussed, and as we show in this letter, they reveal a very unusual behaviour. The aim of the present study of $\text{Pr}_{0.63}\text{Ca}_{0.37}\text{MnO}_3$ is to explore the coupling between phonons, electrons and spins by examining the temperature dependence of Raman linewidths across the CO and magnetic transitions. Our studies do reveal a strong anomalous temperature dependence of the linewidths of the two Raman active A_g modes, which we have quantitatively analysed in terms of strong spin-lattice coupling in these systems.

The single crystal used for the experiment was prepared by the float zone technique [5]. A (100) crystalline face of dimensions 5 mm diameter and 2 mm thickness was polished using diamond paste and mounted on the cold finger of the closed-cycle helium refrigerator (RMC model 22C CRYODYNE) using thermally cycled GE (M/s. General Electric, USA) varnish. Raman spectra were recorded in the spectral range 150 cm^{-1} to 750 cm^{-1} in back-scattering geometry using a DILOR XY spectrometer equipped with a liquid-nitrogen-cooled charge-coupled device detector. An argon ion laser line at 514.5 nm was used as the excitation wavelength at laser power of ~ 25 mW focussed to a spot of 40 μm on the sample. The temperatures quoted are those measured on the cold finger using a Pt-sensor coupled to a home-made temperature controller. The temperatures are within an accuracy of ± 1 K and do not take into account laser heating.

For an ideal perovskite ABO_3 with cubic structure (space group O_h^1 , $Pm\bar{3}m$) the irreducible representations at the zone center are given by $4F_{1u} + F_{2u}$. The only allowed optical modes are the infrared modes and since all lattice sites have inversion symmetry, first-order Raman scattering is forbidden. The small size of the Pr cation in comparison to the oxygen causes a large tilting of the MnO_6 octahedra leading to a GdFeO_3 structure. The space group of $\text{Pr}_{0.63}\text{Ca}_{0.37}\text{MnO}_3$ at room temperature is $Pbnm$ (D_{2h}^{16}); there are four formula units per unit cell and there are 24 Raman active modes [9]. Iliev *et al.* [9] have carried out systematic Raman measurements at room temperature and lattice dynamical calculations on undoped, stoichiometric, orthorhombic YMnO_3 and LaMnO_3 with $Pbnm$ structure and identified the symmetry of the different modes. The Raman modes are weak even in stoichiometric LaMnO_3 ; the observed modes at 140, 198, 257, 284 and 493 cm^{-1} were assigned A_g symmetry, modes

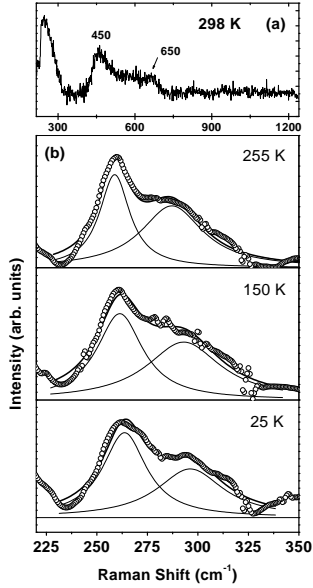


Fig. 1

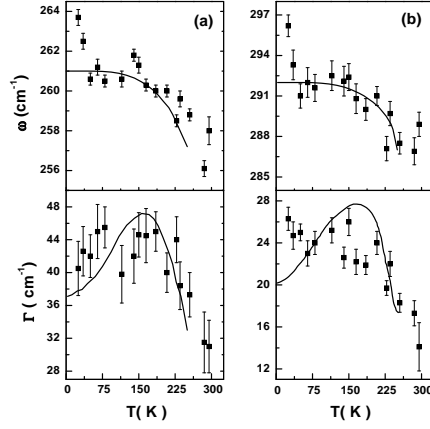


Fig. 2

Fig. 1 – Raman spectra as a function of temperature. (a) Micro-Raman spectrum taken at 298 K showing the modes at ~ 260 , 450, and 650 cm^{-1} . (b) Raman spectrum of $A_g(2)$ and $A_g(4)$ modes at three different temperatures. The thick solid smooth curves show the sum of the two fitted Lorentzian lineshapes (thin solid smooth curve). Raw data has been denoised using a wavelet filtering routine (Daubechies wavelet filter of order 4 at level 4).

Fig. 2 – Variation of the Raman frequency (ω) and the full width at half-maximum (Γ) as a function of temperature. Filled squares are the experimental values and thick solid curves are the theoretical results in our model calculation. Panel (a) is for the $A_g(2)$ mode and panel (b) is for the $A_g(4)$ mode.

at $109, 170, 308, 481$ and 611 cm^{-1} as B_{2g} and modes at 184 and 320 cm^{-1} as B_{1g} or B_{3g} . Recent experiments on LaMnO_3 have revealed the presence of high-energy modes ($\sim 1000 \text{ cm}^{-1}$) which have been attributed to the orbital excitations [17]. However, doped manganites being pseudo-cubic, Raman lines are extremely weak and broad [9–13]. The number of modes observed in doped manganites are very few; *e.g.*, in $\text{La}_{0.7}\text{Ca}_{0.3}\text{MnO}_3$ there are five modes observed at low temperature at $70, 133, 235, 435$, and 670 cm^{-1} [11].

In the micro-Raman setup using 6328 \AA radiation from He-Ne laser, we observe four bands centered around $\sim 260, 290, 450$ and 650 cm^{-1} . However, in macro-geometry with the crystal in the cryostat, only two modes centered around 258 and 288 cm^{-1} at 300 K were observed with sufficient signal to noise ratio (Fig. 1). The other bands near 450 and 650 cm^{-1} are weaker and therefore could not be followed as a function of temperature.

We will now discuss the origin of the observed modes. Since the crystal structure for $\text{Pr}_{1-x}\text{Ca}_x\text{MnO}_3$ is same as that of LaMnO_3 , it is plausible to assign to these modes the

symmetry used by Iliev *et al.* [9] for LaMnO_3 . The low-frequency mode at 258cm^{-1} has been attributed to the $A_g(2)$ mode which is the in-phase rotation of the oxygen cage about the y -axis on adjacent MnO_6 octahedra. In this mode only the in-plane oxygen atoms, namely O1, are involved. The mode at 288cm^{-1} has been assigned to the $A_g(4)$ mode which is out-of-phase rotation of the oxygen cage about the x -axis. Here along with the in-plane oxygens (O1), the apical oxygens (O2) are also involved. The Mn ion being at the centre of inversion symmetry remains stationary in both the modes. Figs. 2a and 2b show the variation of the peak position and linewidths (full width at half-maximum) for the two modes as a function of temperature, obtained by nonlinear least-square fitting of the data with a sum of two Lorentzians along with a baseline. The mode frequencies increase as the temperature is lowered and a sharp change is noticeable at ~ 50 K as the system undergoes a transition to a canted AFI phase [5]. Most interestingly, the linewidths for both the modes show anomalous behaviour in that the widths decrease as the temperature is increased. Another notable observation is the large value of linewidth even at low temperatures.

Next we look at the various possibilities that may lead to the observed temperature dependence of mode frequencies. Mode softening ($\sim 3\%$) as the temperature is raised can arise due to the quasi-harmonic contribution arising from the lattice expansion which can, in turn, change the force constants. This change in frequency is related to the Grüneisen parameter and the volume change. Since the fractional volume change across the studied temperature regime is not available for $\text{Pr}_{0.63}\text{Ca}_{0.37}\text{MnO}_3$ we can be guided by the data available in literature for $\text{Pr}_{0.7}\text{Ca}_{0.3}\text{MnO}_3$. The volume change is $\sim 0.4\%$ between temperatures of 300 and 10 K. This change is too small to account for the observed frequency changes of both the A_g modes. Another contribution can arise due to the intrinsic anharmonic (cubic) interactions. This contribution is also insufficient to explain the large softening, since typically for perovskites, *e.g.*, KTaO_3 , the change of peak position is about $2\text{-}3\text{ cm}^{-1}$ in the temperature range 10-500 K [18].

Now we consider the linewidths. Anharmonic interactions will lead to an increase of the linewidth with increasing temperature, in contrast to our experimental results. Lee and Min [19] have proposed a model to explain the sound velocity softening across the charge ordering transition in $\text{La}_{0.5}\text{Ca}_{0.5}\text{MnO}_3$ [20]. Recently Dattagupta and Sood [21] have extended this model incorporating both the DE interaction and electron-optical phonon coupling. Their models also fail to explain the behaviour of linewidth at low temperatures in the magnetically ordered phase. We suggest that magnon-phonon interaction leads to the shifts in phonon frequencies as well as the observed temperature dependence of lifetimes. The frequency shift can be understood as arising due to the modulation of the exchange integral between Mn ions. This has been considered earlier for $\text{LaMnO}_{3+\delta}$ [13] to explain the softening of the Mn-O-Mn stretching mode. However, this model also does not take into account the dynamics and hence cannot explain the temperature dependence of the linewidth(Γ). A sharp increase in the peak positions at low temperatures near the canted AF transition (see Fig. (2)) suggests a strong coupling between the Raman modes and spin excitations, which we show to be also responsible for the anomalous temperature dependence of the linewidths.

We briefly outline here the origin of the large spin-phonon coupling and the way it leads to anomalous phonon damping. Details will be published elsewhere [22]. When the neighbouring MnO_6 octahedra are tilted, the Mn-O-Mn bond angle $\theta_{ij}(=\pi - (\theta_i - \theta_j))$ between nearest-neighbour Mn-O bonds involving Mn ions i and j changes. Here θ_i and θ_j are the small angles of rotation of the neighbouring octahedra centred at i and j , respectively. Since the oxygen mediated overlap t_{ij} between Mn- d orbitals goes as $\cos\theta_{ij}$, J_{ij} goes as $J_{ij}^0 \cos\theta_{ij}/2 \sim J_{ij}^0(1 - \frac{(\theta_i - \theta_j)^2}{2})$. This has a term of the form $\theta_i\theta_j$ which, among others, corresponds to a

simultaneous excitation of the rotation mode involving the Mn-O bond, with a displacement $q_{1i}(\sim a\theta_i)$ and another mode $q_{2j}(\sim a\theta_j)$ where a is the Mn-O bond length. The coupling between the two phonons will be strongest if they belong to the same symmetry representation. The first of these is the Raman-active phonon under consideration, with a frequency $\omega_1 = 258\text{cm}^{-1}$ ($A_g(2)$) or $\omega_1 = 288\text{cm}^{-1}$ ($A_g(4)$) and the other is an optical phonon mode with frequency ω_2 .

For simplicity in calculation, we assume that the magnetic order is of the C-type in which ferromagnetic chains are linear in contrast to the zig-zag chains in the CE structure. Both these structures are geometrically similar, have the same number of nearest-neighbour FM and AF bonds per spin, and have the same magnetic energies per spin [23]. Though there can be quantitative differences in their magnetic excitation spectrum, qualitatively both are very similar in that they have mixed FM and AF character along arbitrary directions of the Brillouin zone with the same number of nearest-neighbour FM/AF couplings and the same overall geometry, namely FM along a line and AF in plane. The latter decides the dispersion relation and the phase space for the mixed FM and AF spin excitations. Since we are interested in understanding how magnetic fluctuations affect the phonon spectrum, it is therefore a very good approximation to work with the C-type structure rather than the CE or pseudo-CE type structures. The effective spin-Hamiltonian for this anisotropic spin system is given by

$$H_{spin} = \sum_{\langle ij \rangle; i, j \in xz} J_{AF}^{xz} \mathbf{S}_i \cdot \mathbf{S}_j - \sum_{\langle ij \rangle; j \in y} J_F^y \mathbf{S}_i \cdot \mathbf{S}_j, \quad (1)$$

where AF and F refer to antiferromagnetic and ferromagnetic interactions. Our Hamiltonian is most naturally viewed as an effective Hamiltonian with t_{2g} spin degrees of freedom kept explicitly, and all other degrees of freedom (such as e_g electrons, JT coupling between e_g electrons and lattice modes *orthogonal* to those considered here, Hund's rule coupling) integrated out. (This is possible and sensible because the t_{2g} spins are the lowest energy degrees of freedom near and below T_N , as discussed below.) It has been shown by several authors, *e.g.*, Kugel and Khomskii [24], that in LaMnO_3 (which is an insulator experimentally showing JT distortions and ferromagnetic planes coupled antiferromagnetically) the Mn-O-Mn-mediated magnetic interaction is *ferromagnetic* in plane and antiferromagnetic (usual superexchange) perpendicular to it. The latter is indeed due to the same sort of virtual processes involving the Mn-O-Mn bond as the AF superexchange. It has been shown that [24] the JT distortions (and consequent e_g orbital excited states), and the Hund's rule coupling J_H (which enslaves the e_g spins to the t_{2g} spin in the ground state *and* produces an excited state an energy J_H away, with e_g, t_{2g} spins antiparallel) lead to a *ferromagnetic* Mn-O-Mn-mediated in-plane exchange coupling. Thus detailed models involving DE and JT coupling show as briefly mentioned above, that both AF and F coupling between t_{2g} spins necessarily involve Mn-O-Mn overlap. Further, if there are no other low-energy degrees of freedom (*e.g.*, no e_g fermionic low-energy metallic excitations, or orbital fluctuations), then the form of Eq. (1) of the text with the discussed dependence on Mn-O-Mn angle, is *inevitable*. A microscopic theory will relate the J_{ij} to basic parameters of the electron Hamiltonian, but J_{ij} is always second order in the Mn-O-Mn overlap. The only other possible low-energy degrees of freedom in the *insulating phases* of CMR oxides are orbital fluctuations. Here we contend that these are not relevant in the temperature range we are working in because orbital order is already well developed. For small fluctuations of the Mn-O bond angle, from the above discussion, the spin-phonon interaction Hamiltonian (H_{s-p}) becomes

$$H_{s-p} = -\frac{g}{2a^2} \sum_{\langle ij \rangle; i, j \in xz} J_{oAF}^{xz} \mathbf{S}_i \cdot \mathbf{S}_j q_{1i} q_{2j} + \frac{g}{2a^2} \sum_{\langle ij \rangle; j \in y} J_{oF}^y \mathbf{S}_i \cdot \mathbf{S}_j q_{1i} q_{2j}$$

$$+ \sum_{\langle ij \rangle; i, j \in xz} J_{oAF}^{xz} \mathbf{S}_i \cdot \mathbf{S}_j - \sum_{\langle ij \rangle; j \in y} J_{oF}^y \mathbf{S}_i \cdot \mathbf{S}_j, \quad (2)$$

where g is a coupling constant of order unity. The spin degrees of freedom are described in terms of Schwinger bosons (SB) [25] which is an exact representation. It is convenient both below and above the Néel temperature (T_N). Below T_N , the SB Bose condense. The spin-spin interaction in Eq. (2) can be written in terms of boson operators $a_{k\sigma}^\dagger$ in mean-field theory as

$$H_{SB} = H_0 + \sum_{k, \sigma} \omega_k [a_{k\sigma}^\dagger a_{k\sigma} + 1]. \quad (3)$$

Here H_0 is a c-number (with no operators in it unlike the second term which is the Hamiltonian of noninteracting SB) to be determined self-consistently from the free energy, and ω_k is the boson frequency,

$$\omega_k = \sqrt{[(\lambda - J_{oF}^y z_y B_y \gamma_k^y) + \lambda]^2 - (J_{oAF}^{xz} z_{xz} B_{xz} \gamma_k^{xz})^2}. \quad (4)$$

Here, B_{xz} and B_y are the Weiss fields (the SB order parameters), and λ is the temperature dependent stiffness of the SB excitations, to be determined self-consistently from the free energy; $z_{xz}(z_y)$ is the xz plane(y -axis) coordination number, and $\gamma_p = 1/z_p \sum_\delta e^{i\mathbf{k} \cdot \delta}$ ($p = xz$ or y). We choose $J_{oAF}^{xz} \sim 3.9 \text{ meV}$ and $J_{oF}^y \sim 7.8 \text{ meV}$ so as to give $T_N = 175 \text{ K}$.

The spin-phonon interaction in Eq. (2), written in terms of the SB operators, leads to a coupling between the A_g mode being observed, and the second optical phonon mode of wavenumber ω_2 , with the excitation of nearest-neighbour spin fluctuations or boson pairs. We calculate the decay rate for the A_g phonons of frequency $\hbar\omega_1$ in perturbation theory, to second order in H_{s-p} . The phonon decays due to the second-order process which involves the A_g phonon decaying into the second phonon and two Schwinger bosons. The imaginary (real) part of the self-energy Σ determines the decay rate (peak shift) of the Raman-active phonon. Assuming the phonon modes to be dispersionless, the imaginary part of Σ is given by

$$\text{Im } \Sigma = \frac{g^2}{8\pi a^2} \sum_{q, k} f(q, k) \delta(\omega_1 - \omega_2 - \omega_k - \omega_q) [1 + g_{\omega(q+k)} + g_{\omega_2}] [1 + g_{\omega(k)} + g_{\omega(q)}], \quad (5)$$

where $f(q, k)$, the form factor is given by

$$\begin{aligned} f(q, k) = & (J_{oF}^y B_y)^2 p_1 A_1^2 + (J_{oF}^y B_y)(J_{oAF}^{xz} B_{xz}) A_1 (p_2 A_2 + p_3 A_3)/2 \\ & + (J_{oAF}^{xz} B_{xz})^2 (p_4 A_3^2 + p_5 A_2^2 + p_6 A_2 A_3)/4, \end{aligned} \quad (6)$$

p_i are products of Bogoliubov or coherence factors, $g_{\omega(k)}^{-1} = e^{\beta\omega_k} - 1$, $A_1 = 2(\cos q_y + \cos k_y)$, $A_2 = 2(\cos q_x + \cos q_z)$, and $A_3 = 2(\cos k_x + \cos k_z)$.

We find substantial linewidth at $T = 0$, which initially increases with temperature because of thermal availability of two SB states at energy $\hbar(\omega_1 - \omega_2)$. At high temperatures, of order T_N or higher, the spin fluctuation mode softens, and the density of pair excitations at a fixed energy difference $\hbar(\omega_1 - \omega_2)$ decreases as temperature increases. The Weiss fields also decrease with increasing temperature. Thus the $A_g(2)$ phonon decay rate falls. This decrease has been estimated in the SB formalism both below and above T_N (the Bose condensation temperature in that formalism), or in a classical theory for spin dynamics of a Heisenberg spin system specially useful above T_N ; the results above T_N are roughly the same. In the latter theory, one essentially obtains the nearest-neighbour spin-fluctuation frequency spectrum via

classical equations of motion of coupled spin vectors. We show the Schwinger boson results in Fig. 2 for both linewidths and peak positions. Guided by the lattice dynamic studies of Iliev *et al.* [9] on LaMnO_3 , we have taken the A_g phonon at 190cm^{-1} as ω_2 . The qualitative behaviour of Γ and peak positions will not change with another choice of ω_2 . As can be seen, the agreement between the experiment and theory is rather good above 70K. Our approach does not take into account the observed canted AFI state below $T < 50\text{K}$, which may be responsible for the discrepancy between the theory and experiments at low temperatures. The canting of spins leads to FM correlations in an otherwise perfectly ordered AF state which, in turn, modifies the spin excitation spectrum.

In conclusion, our Raman measurements on $\text{Pr}_{1-x}\text{Ca}_x\text{MnO}_3$ ($x = 0.37$) reveal a strong coupling between the spin and lattice degrees of freedom in CO manganites. The large variation of the mode frequency and anomalous behaviour of the linewidths as a function of temperature are understood in terms of spin-phonon interaction. Thus, we believe, our study reveals the striking consequences of the strong interplay between the spin and lattice degrees of freedom in CO manganites.

RG and GVP thank the Council of Scientific and Industrial Research (India) and AKS thanks the Department of Science and Technology (India) for financial support.

REFERENCES

- [1] Y. TOKURA (Editor), *Colossal Magnetoresistive Oxides* (Gordon and Breach, London) 2000.
- [2] C. ZENER, *Phys. Rev.*, **82** (1951) 403; P. W. ANDERSON AND H. HASEGAWA, *Phys. Rev.*, **100** (1955) 675.
- [3] A. J. MILLIS, B. I. SHRAIMAN, AND R. MUELLER, *Phys. Rev. Lett.*, **74** (1995) 5144.
- [4] C. N. R. RAO, A. ARULRAJ, A. K. CHEETHAM, AND B. RAVEAU, *J. Phys.:Condens. Matter*, **12** (2000) R83.
- [5] Y. TOMIOKA *et al.*, *Phys. Rev. B*, **53** (1996) 1689.
- [6] M. R. LEES *et al.*, *Phys. Rev. B*, **52** (1995) R14303; Z. JIRAK *et al.*, *J. Magn. Magn. Mater.*, **15-18** (1980) 519.
- [7] D. E. COX *et al.*, *Phys. Rev. B*, **57** (1998) 3305.
- [8] AYAN GUHA *et al.*, *Phys. Rev. B*, **62** (2000) R11941.
- [9] M. N. ILIEV *et al.*, *Phys. Rev. B*, **57** (1998) 2872.
- [10] J. C. IRWIN, J. CHRZANOWSKI, AND J. P. FRANCK, *Phys. Rev. B*, **59** (1999) 9362.
- [11] V. B. PODOBEDOV *et al.*, *Phys. Rev. B*, **58** (1998) 43.
- [12] S. YOON *et al.*, *Phys. Rev. B*, **58** (1998) 2795.
- [13] E. GRANADO *et al.*, *Phys. Rev. B*, **60** (1999) 11879.
- [14] R. GUPTA *et al.*, *Phys. Rev. B*, **54** (1996) 14899.
- [15] V. DEDIU *et al.*, *Phys. Rev. Lett.*, **84** (2000) 4489.
- [16] V. A. AMELITCHEV *et al.*, *Phys. Rev. B*, **63** (2001) 104430.
- [17] E. SAITOH *et al.*, *Nature*, **410** (2001) 180.
- [18] C. H. PERRY *et al.*, *Phys. Rev. B*, **39** (1989) 8666.
- [19] J. D. LEE AND B. I. MIN, *Phys. Rev. B*, **55** (1997) R14713.
- [20] A. P. RAMIREZ *et al.*, *Phys. Rev. Lett.*, **76** (1996) 3188.
- [21] S. DATTA GUPTA AND A. K. SOOD, *Phys. Rev. B*, **65** (2002) 064405.
- [22] G. VENKETESWARA PAI *et al.*, *unpublished*.
- [23] G. VENKETESWARA PAI, *Phys. Rev. B*, **63** (2001) 064431.
- [24] K. I. KUGEL AND D. KHOMSKII, *Sov. Phys. JETP*, **37** (1973) 725; D. FEINBERG *et al.*, *Phys. Rev. B*, **57** (1998) R5583.
- [25] S. SARKER *et al.*, *Phys. Rev. B*, **40** (1989) 5028.